

NASA Technical Memorandum 83457
AIAA-83-1200

Perspectives on the Mixing of a Row of Jets with a Confined Crossflow

J. D. Holdeman
Lewis Research Center
Cleveland, Ohio

Prepared for the
Nineteenth Joint Propulsion Conference
cosponsored by the AIAA, SAE, and ASME
Seattle, Washington, June 27-29, 1983



PERSPECTIVES ON THE MIXING OF A ROW OF JETS WITH A CONFINED CROSSFLOW

by J.D. Holdeman

NASA Lewis Research Center
Cleveland, OH 44135

Abstract

An interactive computer code, written for a microcomputer, is presented which displays 2-D and 3-D oblique plots of the temperature distribution downstream of jets mixing with a confined crossflow, for either single-side or opposed jet injection. Temperature profiles calculated with this routine are presented to show the effects of flow and geometric variables on the mixing. Examples are also shown to illustrate the different perspectives on the mixing available by exercising various view options. In addition, the program is used to calculate profiles for opposed rows of jets with their centerlines in-line, by assuming that the confining effect of an opposite wall is equivalent to that of a plane of symmetry between opposed jets.

Nomenclature

CD	= orifice discharge coefficient
D	= orifice diameter
Dj	= (D) (SQRT (CD))
DR	= jet-to-mainstream density ratio = T_m/T_j
H	= duct height at injection plane
J	= jet-to-mainstream momentum ratio = $DR(V_j/U_m)^2$
m _J	= jet mass flow rate
m _M	= mainstream mass flow rate
MR	= jet-to-mainstream mass flow ratio = m_J/m_M
m _T	= $m_J + m_M$
PF	= pattern factor = $MR(1-THETA_{min}/TB)$
S	= spacing between orifice centers
T	= temperature
T _j	= jet exit temperature
T _m	= mainstream temperature
TB	= bulk temperature difference ratio = m_J/m_T
THETA	= $(T_m-T)/(T_m-T_j)$ or = $(T-T_j)/(T_m-T_j)$
U	= velocity
U _m	= mainstream velocity
V _j	= jet velocity
X	= downstream coordinate = 0 at injection plane
Y	= cross-stream (radial) coordinate = 0 at wall
Z	= lateral (circumferential) coordinate = 0 at centerplane

Introduction

The problem of jets-in-crossflow has been rather extensively treated in the literature, to the point that it can almost be considered to be a 'classical' three-dimensional flow problem. Although these studies have all contributed additional understanding of the general problem, the information obtained in any given study is determined by the motivating application, and may not satisfy the specific needs of diverse applications.

Considerations of dilution zone mixing in gas turbine combustion chambers, have motivated several investigations of the mixing characteristics of a row of jets injected normally into a flow of a different temperature in a constant area duct (e.g. references 1 to 3). In the combustor dilution zone, for which these experiments were a generic model, rapid mixing of the diluent air with the primary airstream is desired to provide a suitable temperature distribution at the turbine inlet, quench any continuing chemical reactions, and reduce combustor length.

From the data of references 1 and 2, an empirical model was developed (refs. 4 & 5) for predicting the temperature field downstream of a row of jets mixing with a confined crossflow. This paper presents an interactive computer code, based on this model, for evaluation of dilution zone design alternatives. The purpose of this program is to provide an engineering tool to reduce combustor development time and cost by allowing the designer to investigate the effects of varying flow and/or geometric parameters on combustor exit temperature profiles.

Flow Field Model

Figure 1 is a schematic of the flow field. The jets are shown here entering the main flow through orifices in the top duct wall, but this is arbitrary. The primary independent geometric variables are orifice size, and the spacing between adjacent orifices. These are conveniently expressed in dimensionless form as the ratio of the duct height to orifice diameter, H/D, and the ratio of the orifice spacing to orifice diameter, S/D.

Because the designers' objective is to identify orifice configurations to optimize

the mixing within a given combustor length, or to adjust an unacceptable exit plane temperature distribution, the downstream stations of interest are defined in intervals of the duct height, H, rather than the orifice diameter, D.

The independent flow variables are the momentum ratio, J, the density ratio, DR, and the orifice discharge coefficient, CD. These, and the dependent flow and geometric variables are identified in figure 2.

The results for the temperature field are given in three-dimensional oblique views, as shown in figure 3. Here the local temperature is given by the dimensionless temperature difference ratio,

$$\text{THETA} = \frac{(T_m - T)}{(T_m - T_j)}$$

on the abscissa. Note that this parameter is bounded between 0 and 1, with the former representing unmixed mainstream fluid, and the latter unmixed jet fluid.

The ordinate and oblique coordinates are the Y and Z directions, which are respectively normal to and along the orifice row, in a constant-X plane. The Z-distance shown in the oblique plots is twice the orifice spacing for each configuration. The orifices are shown scaled in proportion to the spacing.

Program Options

The present version of this code provides a three-dimensional pictorial representation of the temperature field, as given by the empirical correlations in references 4 and 5. The program, written in BASIC primarily for use on a microcomputer, is menu-driven, and includes an introduction, a flow schematic, a nomenclature listing, a discussion of program options, example plots, and a choice of output options.

Temperature distributions may be calculated at any user-specified downstream location (X), for either single-side or opposed jet injection. Profiles may be shown as 'cold' THETA distributions, as in figure 3, where the numerator is the difference between the local and the undisturbed mainstream temperature, or as 'hot' THETA distributions with the numerator giving the local difference from the jet temperature. Thus, THETA=1 represents unmixed jet fluid in the 'cold' THETA distribution, and unmixed mainstream fluid in the 'hot' THETA distribution. Individual profiles from the oblique view may also be plotted, either separately or overlaid.

Different perspectives on the mixing can be obtained by specifying jet injection from the top, bottom, left, or right duct wall, or with the plane between jets, the midplane, rather than the plane through the

orifice center, the centerplane, at the edge in the oblique view.

For all options, the flow and geometric variables that must be specified are the discharge coefficient, density ratio, momentum ratio, orifice spacing-to-diameter ratio, and duct height-to-orifice diameter ratio. Although calculations can be performed for most flow and geometric conditions of interest, they will be most reliable for conditions within the range of the experiments on which the correlations are based, i.e.

density ratio, DR	1.6 to 2.6
momentum ratio, J	6 to 60
spacing to diameter ratio, S/D	2 to 6
duct height to diameter ratio, H/D	4 to 16

Not all combinations were tested. The experimental results, the empirical model, and comparisons of the model results with the data are presented in references 1, 2, 4, and 5.

The Effects of Flow Conditions and Geometry on the Temperature Profiles

Figures 4 to 10 show example variations in THETA profiles as functions of the independent flow and geometric variables.

Downstream Distance. Figure 4 shows the variation in temperature distributions with downstream distance. The locations shown are X/H = .25, .5, 1, and 2 from left to right across each row. In this figure the momentum ratio and the total orifice area, and hence the jet to mainstream flow ratio, are constant. Thus, the range of temperature distributions from under-penetration in part a) to over-penetration in part b), results entirely from variation in orifice size and spacing at a fixed operating condition.

Momentum Ratio. Figure 5 shows a typical increase in jet penetration with increasing momentum ratio, at a downstream distance equal to one-half duct height. Since the orifice area is constant in this figure, the jet-to-mainstream flow ratio increases with momentum ratio from left to right across the row.

Density Ratio. The analyses of the experimental data in reference 1 suggested that the effect of varying the density ratio was of second order, for flows with a constant momentum ratio. This can be seen in figure 6, where the density ratio varies from .5 to 2 at a momentum ratio of 26.4, for the same orifice geometry and downstream distance as in figure 5.

Spacing. Figure 7 shows the effect of decreasing the lateral spacing between orifices on the temperature distributions at a downstream distance equal to one-half of the duct height. The lateral uniformity

of the profiles increases, and the penetration decreases slightly as a result of the confinement. Note that the jet-to-mainstream flow ratio increases as the spacing decreases, since the orifice size is constant ($H/D=8$ in all cases). The hole size appears to increase because D is scaled on S , rather than H .

Orifice Size at Constant S/D. Figure 8 shows the increased jet penetration, and increased lateral temperature profile gradients that result from increasing the orifice size with the orifice-spacing-to-diameter ratio (S/D) held constant. Note that since these profiles are at a constant downstream distance (X/H), the dimensionless downstream distance expressed in terms of the orifice size (X/D) varies in inverse proportion to the orifice diameter.

Orifice Size at Constant Spacing. In contrast to the profile variations seen in figure 8, the profiles in figure 9, where the orifice spacing (S/H) is held constant as the diameter increases, remain similar. The profiles in the top and bottom rows are at downstream distances equal to one-half and two duct heights respectively. The orifice diameter is doubled going from left to right, resulting in a four-fold increase in the ratio of the jet-to-mainstream flow. The result is that the temperature distributions are shifted to higher THETA values, consistent with the larger dilution air flow, but the shape of the distributions remains similar.

Spacing and Momentum Coupled.

Analysis of the experimental data in references 2 and 5 suggested a coupling between the momentum ratio and the spacing, and led to the conclusion that for a given momentum ratio there exists a value of S/H for which the most efficient mixing occurs, independent of orifice size. This can be stated as:

$$S/H)_{OPT} = \frac{2.5}{\sqrt{J}}$$

The profiles shown in figure 9 represent optimum mixing conditions for a momentum ratio of 26. Figure 10 shows the profiles which result at different momentum ratios, when the orifice spacing is adjusted according to the relation above. The profiles in parts a) and b) are at downstream distances equal to one-half and two duct heights respectively. In all cases, the jet-to-mainstream mass flow ratio is held constant, and hence the final equilibrium temperature is the same. Clearly, similar distributions are obtained over a range of momentum ratios, if J and S/H are correctly coupled. However, it is also evident that flows with smaller momentum ratios (larger spacing) need greater downstream distances to achieve equivalent mixing.

View Options

Plane of Symmetry. Different features may be apparent depending on which plane of symmetry, centerplane or midplane, is at the edge in the oblique plot. As an example, compare the distribution in figure 11, with the midplane at the edge for $S/D = 2.83$, $H/D = 5.66$, and $J = 26.4$, with the distributions in figures 3 to 10, where the centerplane is at the edge.

THETA Definition. The flow also can appear quite different depending on the definition used for the temperature difference ratio. For example, the temperature distribution for the flow condition in figure 11 is shown in figure 12 in the 'hot' THETA format, where the jet fluid appears as depressions in the distribution.

Injection location. Figure 13 shows two additional views of the temperature difference ratio profiles for $S/D = 2.83$, $H/D = 5.66$, and $J = 26.4$. These profiles are 'cold' THETA distributions with the jets injected from the bottom and front duct walls in parts a) and b) respectively.

Opposed Jet Injection. Finally, the model was used to calculate profiles for opposed rows of jets with their centerlines in-line, by assuming, based on the experimental results of reference 3, that the confining effect of an opposite wall is similar to that of a plane of symmetry between opposed jets. These profiles, for a momentum ratio of 26.4, with $S/D = 2.83$ and $H/D = 11.3$, are shown in figure 14, for downstream distances from $X/H = .25$ to 2. Note that these are for the same momentum ratio and orifice area as the one-side injection profiles in figure 11.

Conclusions

An interactive computer code, written in BASIC primarily for use on a microcomputer, is presented which displays 2-D and 3-D oblique plots of the temperature distribution downstream of jets mixing with a confined crossflow, for either single-side or opposed jet injection.

Temperature profiles calculated with this program are presented to show the effects of flow and geometric variables on the mixing. These confirm the conclusions reached previously (refs. 2 & 5) from examination of the experimental data that:

- 1) mixing improves with downstream distance
- 2) momentum ratio is the most significant flow variable
- 3) the effect of density ratio is small at constant momentum ratio

- 4) decreasing spacing at constant orifice diameter reduces penetration and increases lateral uniformity
- 5) increasing orifice diameter at a constant ratio of spacing to diameter improves penetration but increases lateral non-uniformity
- 6) increasing orifice diameter at constant spacing increases the magnitude of the temperature difference, but jet penetration and profile shape remain similar
- 7) similar distributions may be obtained over a range of momentum ratios, independent of orifice diameter, if spacing and momentum are correctly coupled
- 8) smaller momentum ratios (larger spacing) require a greater distance for equivalent mixing

Examples are presented showing the different perspectives on the mixing obtained with jet injection from the top, bottom, front, and rear duct walls; with the centerplane rather than the midplane at the edge in the 3-D plot; and with a 'hot', $(T-T_j)/(T_m-T_j)$, rather than a 'cold', $(T_m-T)/(T_m-T_j)$, THETA definition. In addition, the model is used to calculate profiles for opposed rows of jets with their centerlines in-line, by assuming that the confining effect of an opposite wall is similar to that of a plane of symmetry between opposed jets.

References

1. Walker, R.E. and Kors, D.L., "Multiple Jet Study Final Report," NASA CR-121217, June 1973.
2. Holdeman, J.D., Walker, R.E., and Kors, D.L., "Mixing of Multiple Dilution Jets with a Hot Primary Airstream for Gas Turbine Combustors," AIAA Paper 73-1249, Nov. 1973.
3. Kamotani, Y. and Greber, I., "Experiments on Confined Turbulent Jets in Cross Flow," NASA CR-2392, Mar. 1974.
4. Walker, R.E. and Eberhardt, R.G., "Multiple Jet Study Data Correlations," NASA CR-134795, Apr. 1975.
5. Holdeman, J.D. and Walker, R.E., "Mixing of a Row of Jets with a Confined Crossflow," *AIAA Journal*, Vol. 15, No. 2, Feb. 1977, pp243-249.

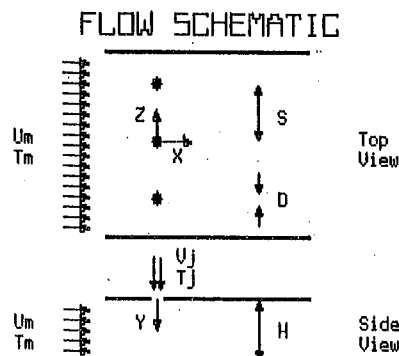


Figure 1. Flow Schematic

Independent Variables

$DR = T_m/T_j$
 $J = DR \langle U_j/U_m \rangle^2$
 CD discharge coefficient
 S/D
 H/D
 X/H

Dependent Variables

temperature
 $NR = m_j/m_H$
 $TB = m_j / (m_H + m_j)$
 $PF = NR (1 - THETA_{min}/TB)$
 S/H
 X/D

Figure 2. Independent and Dependent Variables

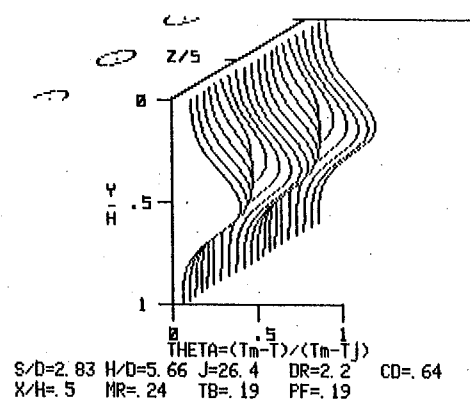


Figure 3. Typical 3-D Oblique Temperature Difference Ratio (THETA) Plot

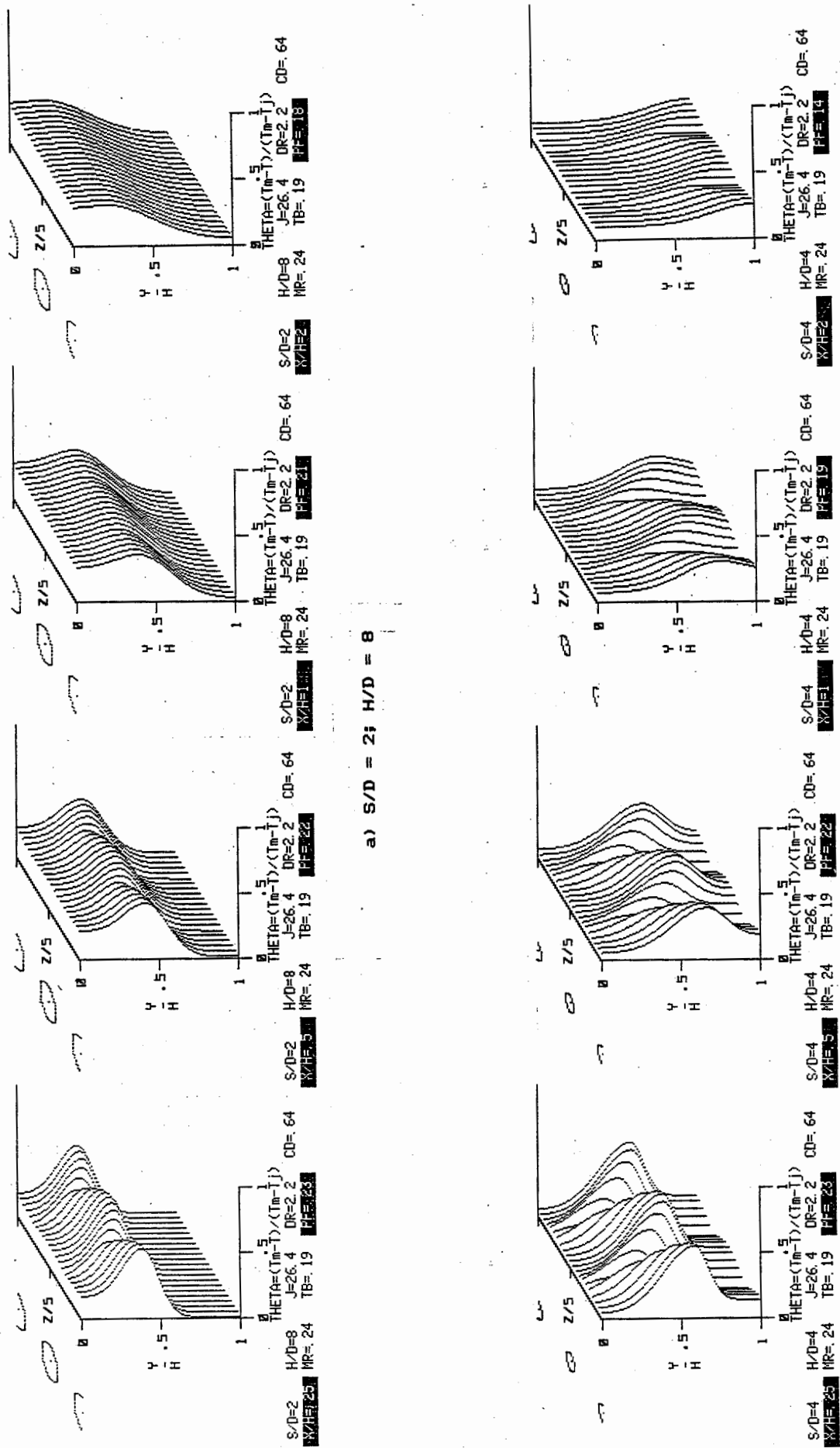


Figure 4. Variation in Temperature Distribution with Increasing Downstream Distance.
J=26.4, DR=2.2, CD=64; MR=24, TB=19

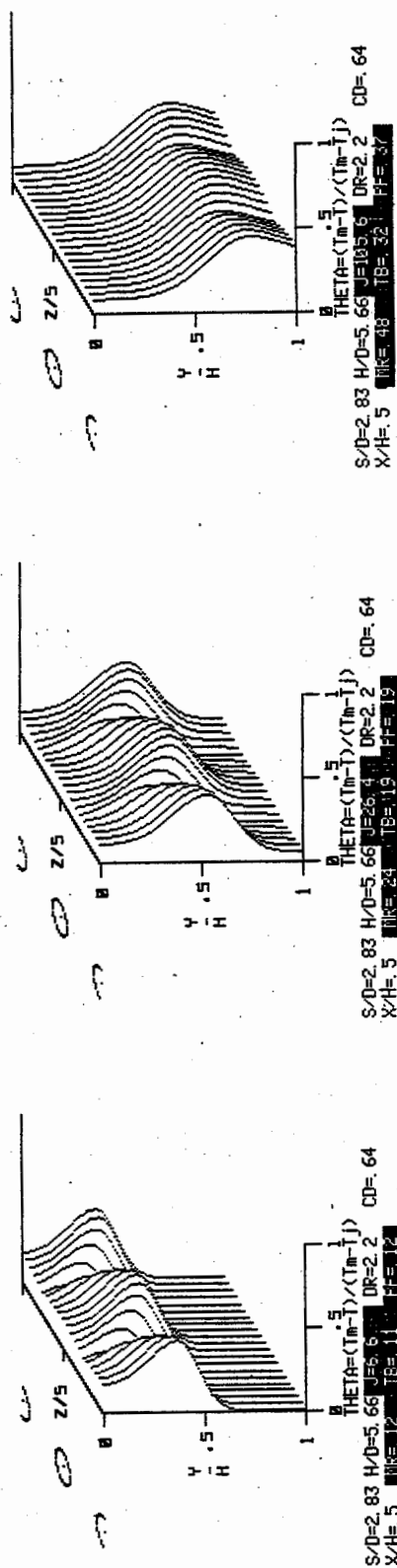


Figure 5. Variation in Temperature Distributions with Increasing Momentum Ratio.
DR=2.2, CD=.64, S/D=2.83, H/D=5.66, X/H=.5

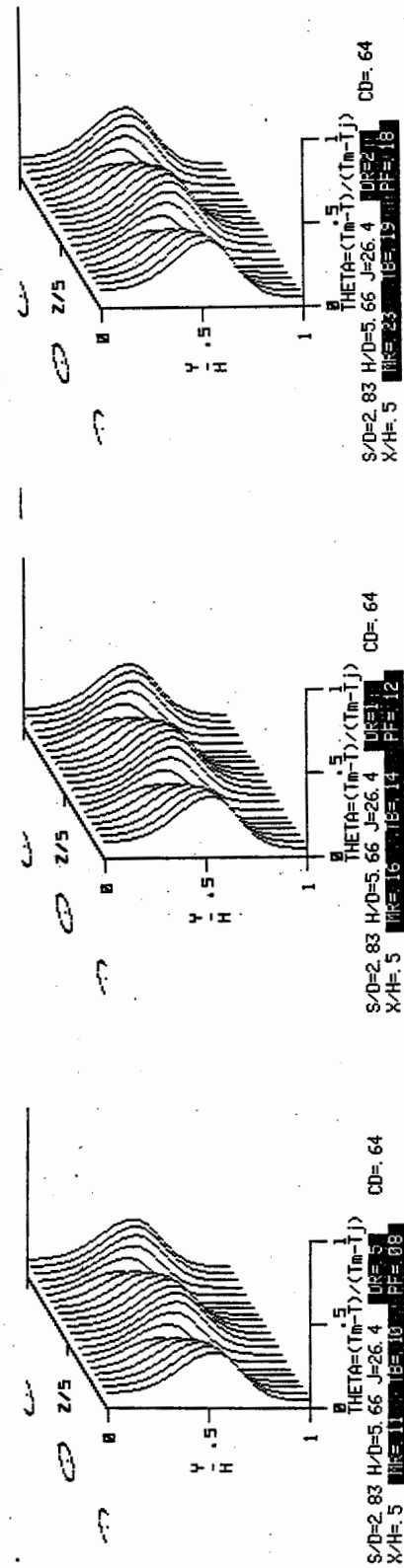


Figure 6. Variation in Temperature Distributions with Increasing Density Ratio.
J=26.4, CD=.64, S/D=2.83, H/D=5.66, X/H=.5

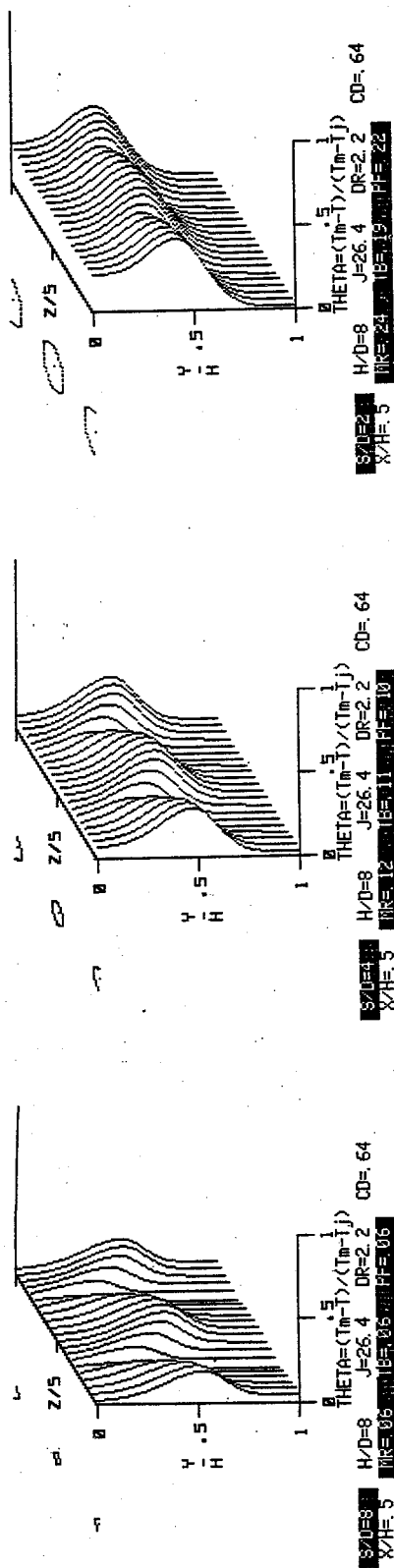


Figure 7. Variation in Temperature Distributions with Decreasing Spacing.

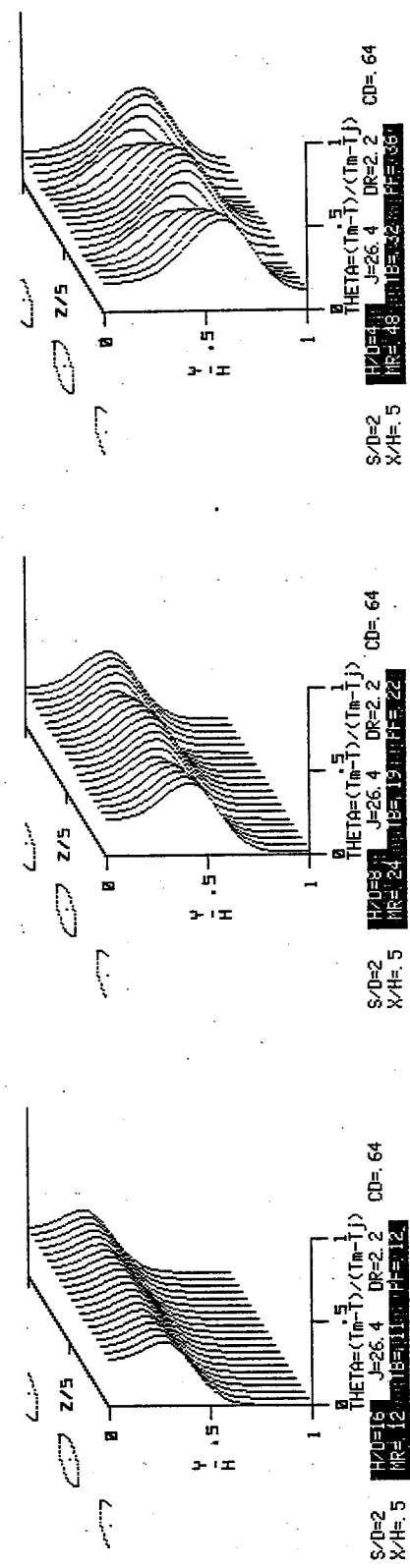
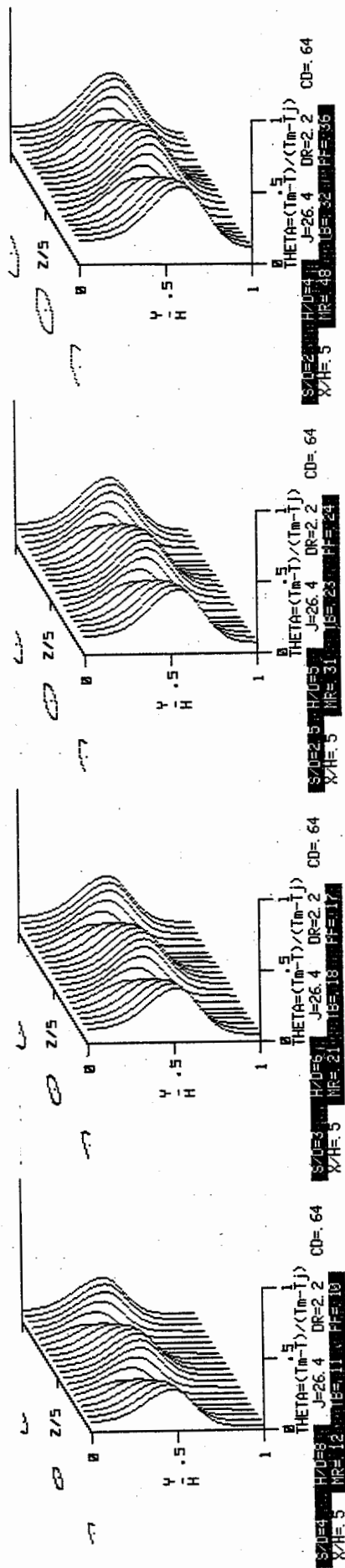
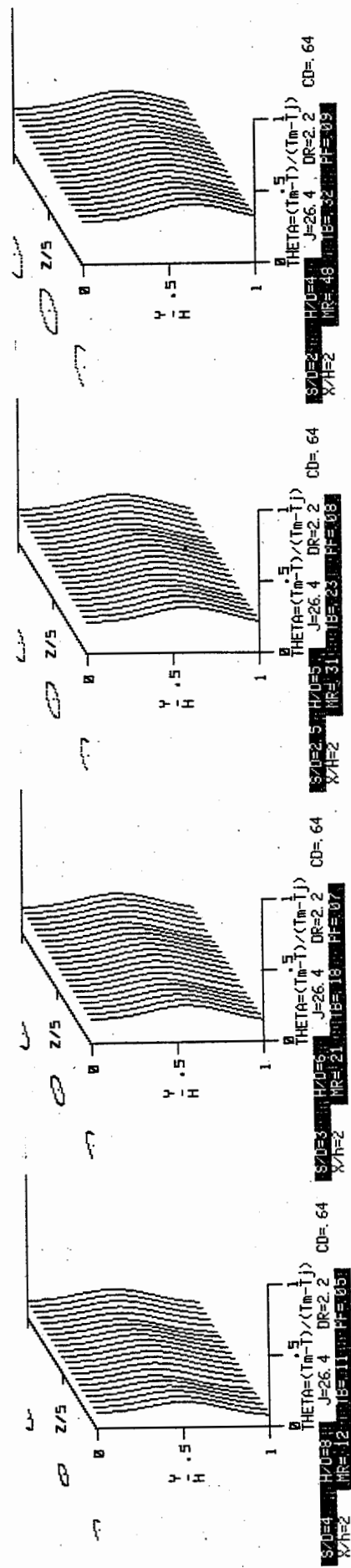


Figure 8. Variation in Temperature Distributions with Increasing Orifice Diameter at Constant S/D.

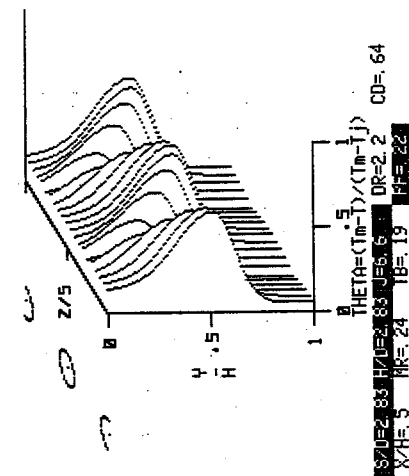
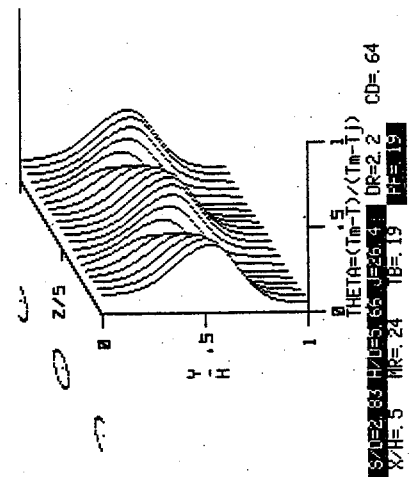
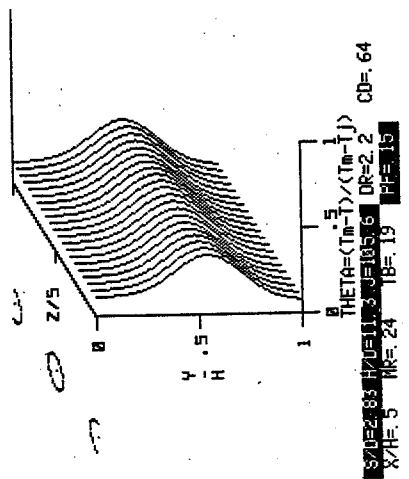


a) $X/H = 0.5$

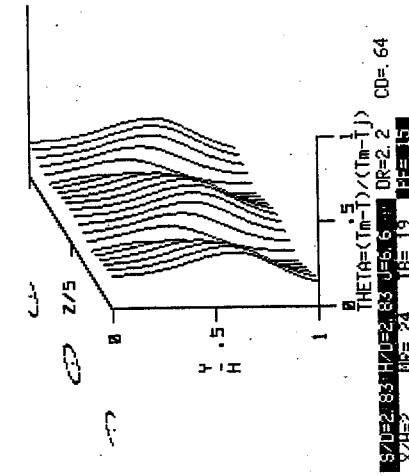
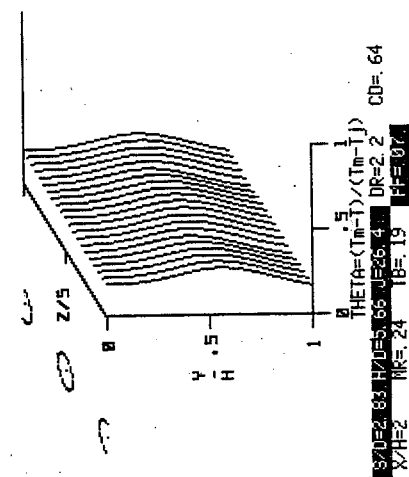
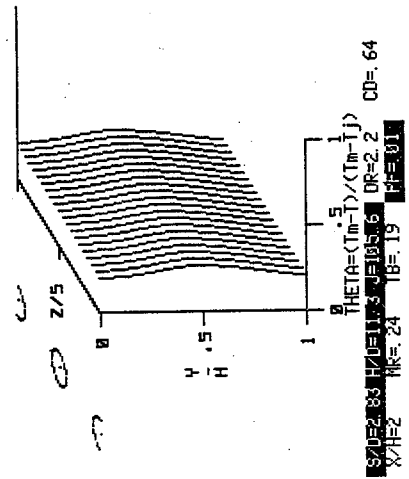


b) $X/H = 2$

Figure 9. Variation in Temperature Distributions with Increasing Orifice Diameter at Constant Spacing. $S/H=0.5$, $J=26.4$, $DR=2.2$, $CD=64$



a) $X/H = 0.5$



b) $X/H = 2$

Figure 10. Variation in Temperature Distributions with Spacing and Momentum Coupled. $S/H=2.5/\sqrt{J}$; $S/D=2.83$, $DR=2.2$, $CD=.64$

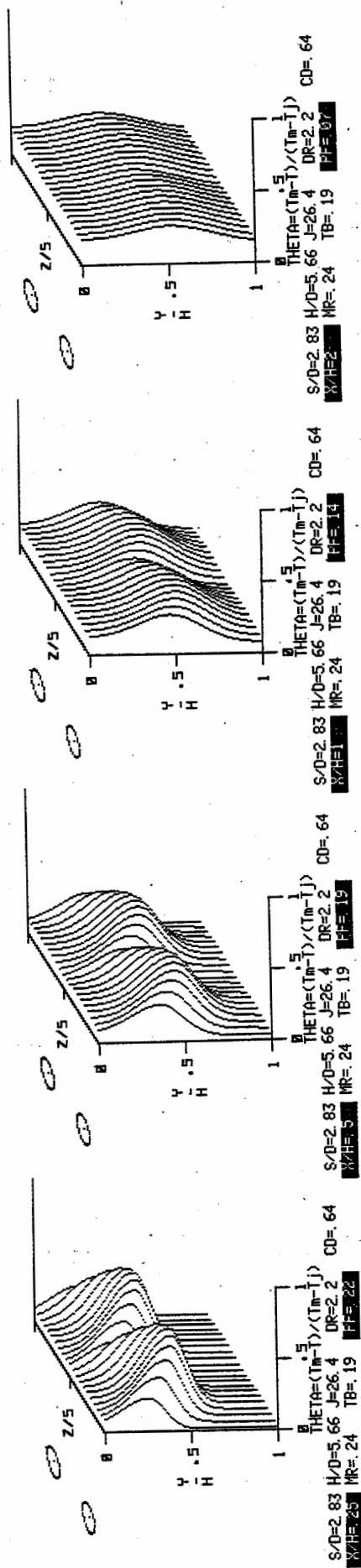


Figure 11. Temperature distributions for top injection and midplane at edge. $S/D=2.83$, $H/D=5.66$, $J=26.4$, $DR=2.2$, $CD=.64$

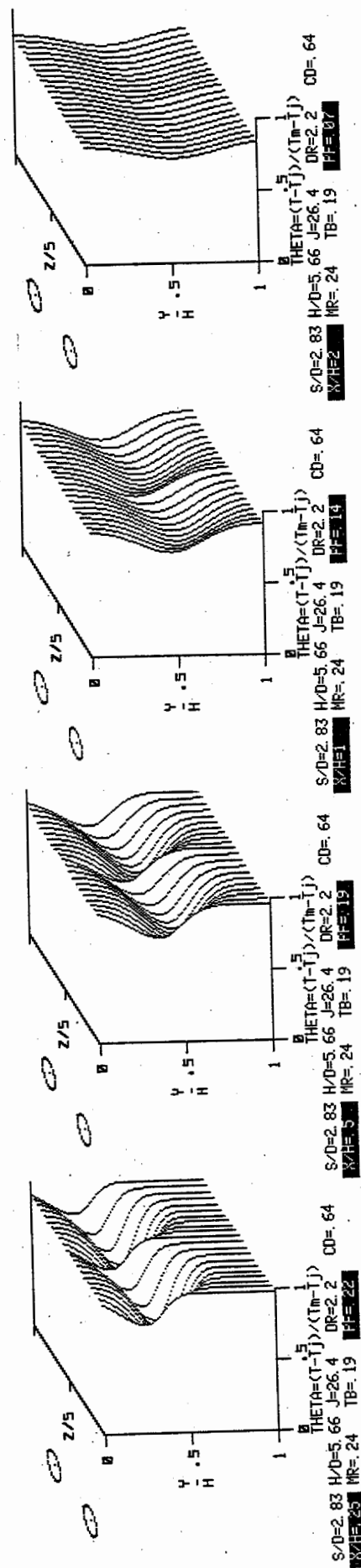


Figure 12. "Hot" θ Temperature distributions for top injection $S/D=2.83$, $H/D=5.66$, $J=26.4$, $DR=2.2$, $CD=.64$

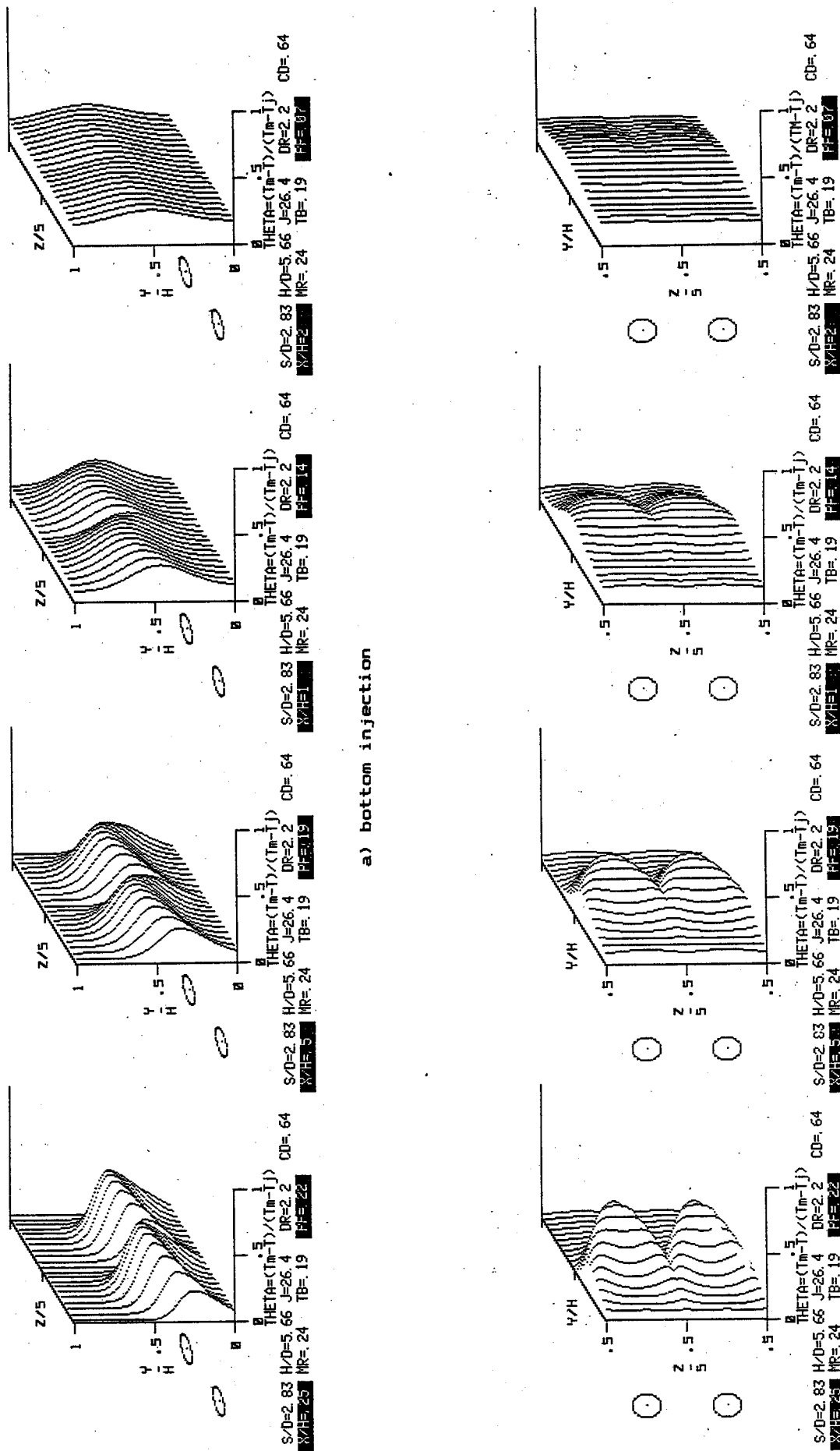


Figure 13. Effect of Varying Side-wall Injection Location on Observed Profiles
 $S/D=2.83$, $H/D=5.66$, $J=26.4$, $DR=2.2$, $CD=64$; $MR=.24$, $TB=.19$, $PF=.19$

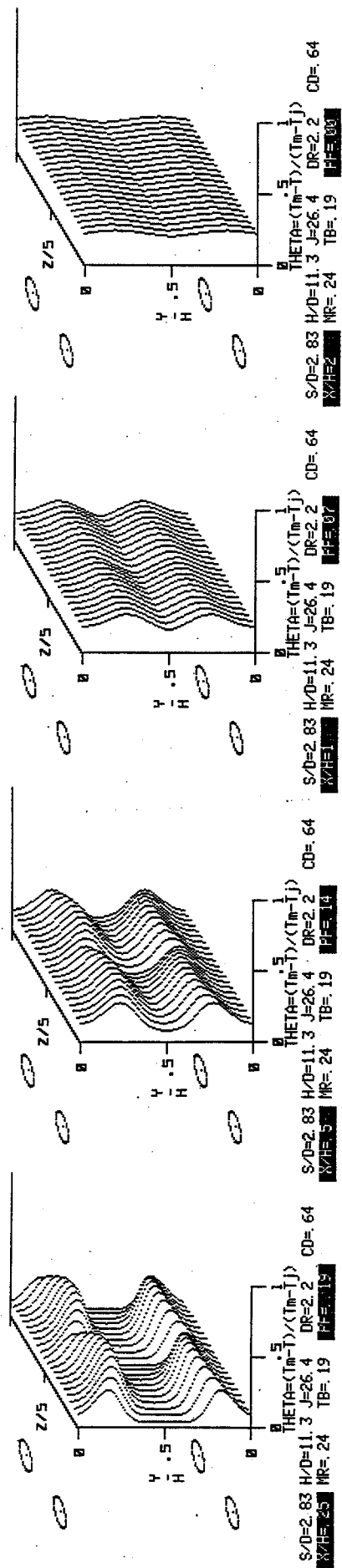


Figure 14. Temperature distributions for opposed jet injection.
S/D=2.83, H/D=11.3, J=26.4, DR=2.2, CD=64

REPORT DOCUMENTATION PAGE			Form Approved OMB No. 0704-0188	
Public reporting burden for this collection of information is estimated to average 1 hour per response, including the time for reviewing instructions, searching existing data sources, gathering and maintaining the data needed, and completing and reviewing the collection of information. Send comments regarding this burden estimate or any other aspect of this collection of information, including suggestions for reducing this burden, to Washington Headquarters Services, Directorate for Information Operations and Reports, 1215 Jefferson Davis Highway, Suite 1204, Arlington, VA 22202-4302, and to the Office of Management and Budget, Paperwork Reduction Project (0704-0188), Washington, DC 20503.				
1. AGENCY USE ONLY (Leave blank)	2. REPORT DATE June 1983	3. REPORT TYPE AND DATES COVERED Technical Memorandum		
4. TITLE AND SUBTITLE Perspectives on the Mixing of a Row of Jets With a Confined Crossflow		5. FUNDING NUMBERS WU-533-04-1A-00		
6. AUTHOR(S) J.D. Holdeman				
7. PERFORMING ORGANIZATION NAME(S) AND ADDRESS(ES) National Aeronautics and Space Administration Lewis Research Center Cleveland, Ohio 44135-3191		8. PERFORMING ORGANIZATION REPORT NUMBER E-1772		
9. SPONSORING/MONITORING AGENCY NAME(S) AND ADDRESS(ES) National Aeronautics and Space Administration Washington, DC 20546-0001		10. SPONSORING/MONITORING AGENCY REPORT NUMBER NASA TM-83457 AIAA-83-1200		
11. SUPPLEMENTARY NOTES Prepared for the Nineteenth Joint Propulsion Conference cosponsored by the AIAA, SAE, and ASME, Seattle, Washington, June 27-29, 1983. Responsible person, James D. Holdeman, organization code 5830, (216) 433-5846.				
12a. DISTRIBUTION/AVAILABILITY STATEMENT Unclassified - Unlimited Subject Category: 02 This publication is available from the NASA Center for AeroSpace Information, (301) 621-0390.		12b. DISTRIBUTION CODE		
13. ABSTRACT (Maximum 200 words) An interactive computer code, written for a microcomputer, is presented which displays 2-D and 3-D oblique plots of the temperature distribution downstream of jets mixing with a confined crossflow, for either single-side or opposed jet injection. Temperature profiles calculated with this routine are presented to show the effects of flow and geometric variables on the mixing. Examples are also shown to illustrate the different perspectives on the mixing available by exercising various view options. In addition, the program is used to calculate profiles for opposed rows of jets with their centerlines in-line, by assuming that the confining effect of an opposite wall is equivalent to that of a plane of symmetry between opposed jets.				
14. SUBJECT TERMS Jets in crossflow; Dilution zone; Jet mixing; Confined jets			15. NUMBER OF PAGES 14	
			16. PRICE CODE A03	
17. SECURITY CLASSIFICATION OF REPORT Unclassified	18. SECURITY CLASSIFICATION OF THIS PAGE Unclassified	19. SECURITY CLASSIFICATION OF ABSTRACT Unclassified	20. LIMITATION OF ABSTRACT	